Electronic Supplementary Information

Calculation method

First-principles calculations are performed using the Vienna Ab initio Simulation Package (VASP) to investigate the NITRR process on the t-$Zr_{0.9}Sc_{0.1}O_{2-\delta}$ (011) surface.[1-4] The valence-core electrons interactions are treated by Projector Augmented Wave (PAW) potentials and the electron exchange correlation interactions are described by the generalized gradient approximation (GGA) with the Perdew-Burke-Ernzerhof (PBE) functional.[5-6] Considered long-range interaction at the interface, Van der Waals interactions are considered using DFT-D3 correlation.[7] To avoid interaction from other slabs, a vacuum of 20 Å is added along z direction. The convergence criterion of geometry relaxation is set to 0.03 eV•$Å^{-1}$ in force on each atom. The energy cutoff for plane wave-basis is set to 500 eV. The K points are sampled with 3×3×1 by Monkhorst-Pack method.[8]

Gibbs free energy change (ΔG) is evaluated based on the computational hydrogen electrode (CHE) model, which takes one-half of the chemical potential of gaseous hydrogen under standard conditions as the free energy of the proton-electron pairs. ΔG is calculated by the following equation[9]:

$$\Delta G = \Delta E + \Delta E_{ZPE} - T\Delta S + neU$$

where ΔE, ΔE_{ZPE}, ΔS are the reaction energy from DFT calculation, the correction of zero-point energy and the change of simulated entropy, respectively. T is the temperature (T = 300 K). *n* and U are the number of transferred electrons and applied potential respectively.

Experimental Method

Materials： Disodium phosphate (Na_2HPO_4), sodium dihydrogen phosphate (NaH_2PO_4), Zirconium acetate ($C_8H_{12}O_8Zr$), Scandium(III) nitrate hydrate ($Sc(NO_3)_3 \cdot xH_2O$), and polyvinylpyrrolidone (PVP) are purchased from Aladdin Ltd (Shanghai, China). Sulfanilamide ($C_6H_8N_2O_2S$) is bought from Heowns technology

Co., Ltd. N,N-Dimethylformamide (DMF), sodium nitrate ($NaNO_3$), sodium nitrite ($NaNO_2$), N- (1-naphthyl) ethyl diamine dihydrochloride ($C_{12}H_{14}N_2.2(HCl)$), phosphoric acid (H_3PO_4), ammonium chloride (NH_4Cl), sodium hypochlorite solution (NaClO), 4-dimethylaminobenzaldehyde ($C_9H_{11}NO$), sodium nitroferricyanide dihydrate ($C_5FeN_6Na_2$-O·$2H_2O$), hydrazine monohydrate ($N_2H_4·H_2O$), hydrogen peroxide (H_2O_2, 3 wt%), hydrochloric acid (HCl), sulfuric acid (H_2SO_4), sodium hydroxide (NaOH), salicylic acid ($C_7H_6O_3$), trisodium citrate dihydrate ($C_6H_5Na_3O_7$-$2H_2O$) and ethanol (C_2H_5OH) are purchased from Kelong chemical Ltd (Chengdu, China). Sodium salicylate ($C_7H_5NaO_3$) is purchased from Fuchen chemical reagents Co., Ltd (Tianjin, China). Nafion solution (5 wt%) is purchased from Sigma-Aldrich Chemical Reagent Co., Ltd. Deionized water is purified through a Millipore system.

Synthesis of t-$Zr_{0.9}Sc_{0.1}O_{2-\delta}$ nanofibers: 1.6 g of PVP (Mw=1,300,000 g mol^{-1}) and 0.05 g of $Sc(NO_3)_3·xH_2O$ were dissolved in 8 mL DMF and 3.07 mL $C_8H_{12}O_8Zr$ (a volume ratio of 8:2), and then this viscous solution was uniformly stirred for 12 h. After that, the mixture was spun into nanofibers at a high voltage of 15 kV. After electrospinning, the fibers were collected and heat treated at 350 °C for 1 h and consecutively sintered at 600 °C for 3 h, which were then naturally cool to room temperature to get the t-$Zr_{0.9}Sc_{0.1}O_{2-\delta}$ nanofibers.

Synthesis of mt-$Zr_{0.9}Sc_{0.1}O_{2-\delta}$ nanofibers: 1.6 g of PVP (Mw=1,300,000 g mol^{-1}) and 0.05 g of $Sc(NO_3)_3·xH_2O$ were dissolved in 8 mL DMF and 3.07 mL $C_8H_{12}O_8Zr$ (a volume ratio of 8:2), and then this viscous solution was uniformly stirred for 12 h. After that, the mixture was spun into nanofibers at a high voltage of 15 kV. After

electrospinning, the fibers were collected and heat treated at 350 °C for 1 h and consecutively sintered at 800 °C for 3 h, which were then naturally cool to room temperature to get the mt-$Zr_{0.9}Sc_{0.1}O_{2-\delta}$ nanofibers.

Synthesis of m-$Zr_{0.9}Sc_{0.1}O_{2-\delta}$ nanofibers: 1.6 g of PVP (Mw=1,300,000 g mol^{-1}) and 0.05 g of $Sc(NO_3)_3 \cdot xH_2O$ were dissolved in 8 mL DMF and 3.07mL $C_8H_{12}O_8Zr$ (a volume ratio of 8:2), and then this viscous solution was uniformly stirred for 12 h. After that, the mixture was spun into nanofibers at a high voltage of 15 kV. After electrospinning, the fibers were collected and heat treated at 350 °C for 1 h and consecutively sintered at 1200 °C for 3 h, which were then naturally cool to room temperature to get the m-$Zr_{0.9}Sc_{0.1}O_{2-\delta}$ nanofibers.

Synthesis of ZrO_2 nanofibers: 1.4 g of PVP (Mw=1,300,000 g mol^{-1}) was dissolved in 8 mL DMF and 2 mL $C_8H_{12}O_8Zr$ (a volume ratio of 8:2), and then this viscous solution was uniformly stirred for 12 h. After that, the mixture was spun into nanofibers at a high voltage of 15 kV. After electrospinning, the fibers were collected and heat treated at 350 °C for 1 h and consecutively sintered at 800 °C for 3 h, which were then naturally cooled to room temperature to get the ZrO_2 nanofibers.

Synthesis of mt-ZrO_2 nanofibers: 1.4 g of PVP (Mw=1,300,000 g mol^{-1}) was dissolved in 8 mL DMF and 2 mL $C_8H_{12}O_8Zr$ (a volume ratio of 8:2), and then this viscous solution was uniformly stirred for 12 h. After that, the mixture was spun into nanofibers at a high voltage of 15 kV. After electrospinning, the fibers were collected and heat treated at 350 °C for 1 h and consecutively sintered at 600 °C for 3 h, which were then naturally cooled to room temperature to get the mt-ZrO_2 nanofibers.

Material characterizations： X-ray diffraction (XRD) analysis was performed by a Rigaku Smartlab with the radiation of Cu Kα. The sample morphology was photographed by ZEISS Gemini SEM 300 scanning electron microscope. The acceleration voltage was 3 kV during topography shooting and 15 kV during energy spectrum mapping shooting. The detector is SE2 secondary electronic detector. The transmission electron microscopy (TEM) and high-resolution TEM (HRTEM) images of sample were obtained using FEI F30 equipment with the accelerating voltage of 300 kV. X-ray photoelectron spectrometer (Thermo Fischer, ESCALAB Xi+) was used for XPS test. The excitation source was Al Kα ray (hv =1486.6 eV), and the working voltage was 12.5 kV. The ion chromatography (IC) was tested by Thermo Scientific ICS-900. Nuclear magnetic resonance (NMR) was measured on a Bruker 400 MHz instrument. The Differential Electrochemical Mass Spectrometry (DEMS) measurements were performed on the Linglu QAS 100.

Working electrode preparation: 5 mg of catalysts were ground into powder and added into a mixed solution containing 660 μL ethanol, 300 μL deionized water and 40 μL of 5 wt% Nafion solution, followed by 30 min ultrasonic dispersion to form a homogeneous suspension. Then, 20 μL of such suspension was dropped on a 1′1 cm^2 carbon paper and dried at ambient temperature.

Electrochemical measurements: All electrochemical tests were performed in an H cell with a Nafion membrane in the middle. A three-electrode system was used in the experiments. The working electrode was carbon sheet coated with catalyst, and the counter electrode was platinum tablet. The electrolyte of the anode was the same as that

of the cathode. The reference electrode was saturated with Ag/AgCl/KCl. The neutral electrolyte was 0.1 M PBS (prepared by Na_2HPO_4 and NaH_2PO_4) solution with pH=7. $NaNO_3$ was added to the electrolyte after high temperature impurity removal as the N source.

In 0.1 M PBS with 0.1 M $NaNO_3$ electrolyte, the voltage of the relative reference electrode (Ag/AgCl) was converted into the voltage of the relatively reversible hydrogen electrode (RHE) by formula (1):

$$E(RHE) = 0.0591 \times PH + E(Ag/AgCl) + 0.197\,V \quad (1)$$

Linear sweep voltammetry (LSV) was used to compare the same electrolyte with and without nitrate at 5 mV s^{-1} scanning speed. Meanwhile, since nitrate concentration had a significant impact on NITRR process, LSV in the same electrolyte with different concentrations of nitrate was tested. Cyclic voltammetry (CV) tests were performed from 0.69 V to 0.79 V vs. RHE at different scan rates of 100 mV s^{-1}, 120 mV s^{-1}, 140 mV s^{-1}, 160 mV s^{-1}, 180 mV s^{-1} and 200 mV s^{-1} without faradaic current. Solution resistance was determined by electrochemical impedance spectroscopy (EIS) at frequencies ranging from 0.1 to 10 kHz.

Determination of ammonia (NH_3): Ammonia produced in the NITRR process was colored by indophenol blue method and detected by the UV-vis spectroscopy. Due to the high concentration of the product, all electrolytes after electrolysis were diluted 10~40 times before color development. After 1 hour of electrolysis, 2 mL of electrolyte was taken from the cathode cell, followed by 2 mL colorant (containing salicylic acid, sodium citrate and sodium hydroxide), 1 mL of oxidant (0.05 M sodium hypochlorite),

and 0.2 mL of catalyst solution (1 wt% sodium nitroferricyanide). Then, they were placed in the dark environment for 1 h, and the UV-vis spectra were measured in the wavelength range of 550 ~ 800 nm. The absorption intensity at 655 nm was substituted into the standard curve to quantify the ammonia yield.

Determination of nitrite (NO_2^-): The concentration of nitrite was measured by Griess reagent. 0.2 g of N- (1-naphthyl) ethyl-diamine dihydrochloride, 2.0 g of sulfa and 5.88 mL of phosphoric acid were dissolved in 100 mL of deionized water, and the Griess reagent was formed after being evenly stirred. After diluting the reacted electrolyte 10-20 times, 1 mL of the diluted electrolyte was taken by addition of 1 mL of Griess reagent and 2 mL of deionized water, and develop color stands in the dark environment of room temperature for 10 minutes. Magenta solution was obtained and UV-vis absorption spectra were tested in the ranges from 400 to 650 nm. The absorbance at 540 nm was substituted into the standard curve to obtain the concentration of nitrite.

Determination of hydrogen (H_2): In the NITRR process, HER is a competitive reaction in cathode. H_2 is the product of HER process and can be detected by blowing the product after electrolysis in the cathode chamber into a gas chromatograph (GC). In order to reduce the experimental error caused by the different thermal conductivity of the gas, the carrier gas of the chromatography is nitrogen. Nitrogen was passed into the cathode electrolyte at a flowing rate of 30 mL min^{-1}, and GC was used to collect the gas produced by the reaction in the cathode chamber every 5 minutes. The hydrogen concentration was obtained by integrating the characteristic peaks of hydrogen

collected in the TCD detector.

Calculations of faradaic efficiency (FE) and yield rate: The yields of NH_3 and NO_2^- are calculated by equation (3):

$$Yield = C \times V \div (t \times m_{cat.}) \quad (3)$$

The FE of NH_3 is calculated by equation (4):

$$FE_1 = 8 \times F \times C(NH_3) \times V \div (17 \times Q) \quad (4)$$

The FE of NO_2^- is calculated by equation (5):

$$FE_2 = 2 \times F \times C(NO_2^-) \times V \div (46 \times Q) \quad (5)$$

The concentration of H_2 is measured by GC and TCD. The volume mole number n can be calculated according to formula (6):

$$n = P \times V' \div (R \times T) \quad (6)$$

The corresponding FE of H_2 can be calculated by equation (7):

$$FE_3 = n \times [H_2] \times F \times 2 \div Q \quad (7)$$

where C is the measured NH_3/NO_2^- concentration, V the volume of electrolyte in the cathode chamber, t the time for which the potential is applied, $m_{cat.}$ the mass of catalyst loaded on the working electrode, F the Faraday constant (F=96485 C mol^{-1}), Q the charge applied, P the standard atmospheric pressure, V' the volume of gas through GC, R the universal gas constant, T the reaction temperature.

^{15}N isotope labeling experiments: $Na^{15}NO_3$ was used as N source for nitrate reduction isotope labeling experiment to verify the origin of as-synthesized ammonia. The purity of $Na^{15}NO_3$ was more than 98.5% and they were stored in a vacuum drying

oven before being used. 0.1 M $Na^{15}NO_3$+0.1 M PBS as the electrolyte, the catalyst was subjected to ^{15}NITRR for 20 h at the optimum voltage. To prepare the NMR sample, the pH of the electrolyte was adjusted to about 1 with 1 M H_2SO_4, then 0.5 mL electrolyte was added with 0.01 vol% DMSO and 0.1 mL D_2O, respectively. The ^{1}H NMR spectrum of $^{15}NH_4^+$ (400 MHz) was determined. As a control, ^{1}H NMR spectrum was tested after reaction in 0.1 M $Na^{14}NO_3$+0.1 M PBS electrolyte.

Differential Electrochemical Mass Spectrometry (DEMS) measurements: PBS solution with 0.1M $NaNO_3^-$ as electrolyte was injected into an electrochemical cell through a peristaltic pump. Ar was then bubbled into the electrolyte at 0.8mL min^{-1} constantly before and during the DEMS test. Carbon paper coated with FTO-E electrocatalysts was used as the working electrode, Pt wire as the counter electrode, Ag/AgCl as the reference electrode. LSV technology was employed from 0.4 V vs. RHE to -1.4 V vs. RHE at a scan rate of 10 mV s^{-1} until the baseline was steady. Then, the corresponding mass signals were collected. After the electrochemical tests were completed and mass signals returned to the baseline, the next circle of test was conducted under the same testing conditions to avoid unexpected errors. After four cycles, the DEMS test was completed.

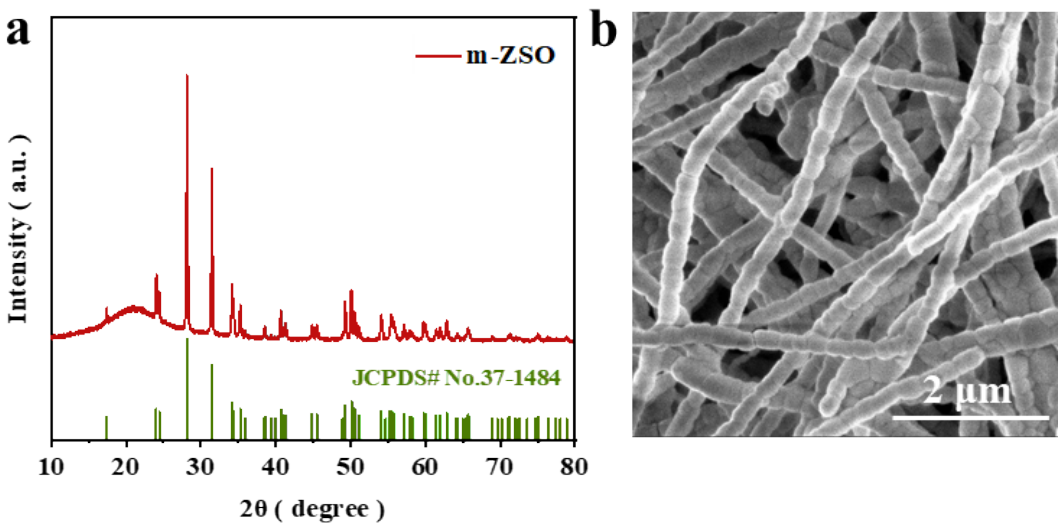

Fig. S1 (a) XRD pattern and (b) SEM image of m-ZSO.

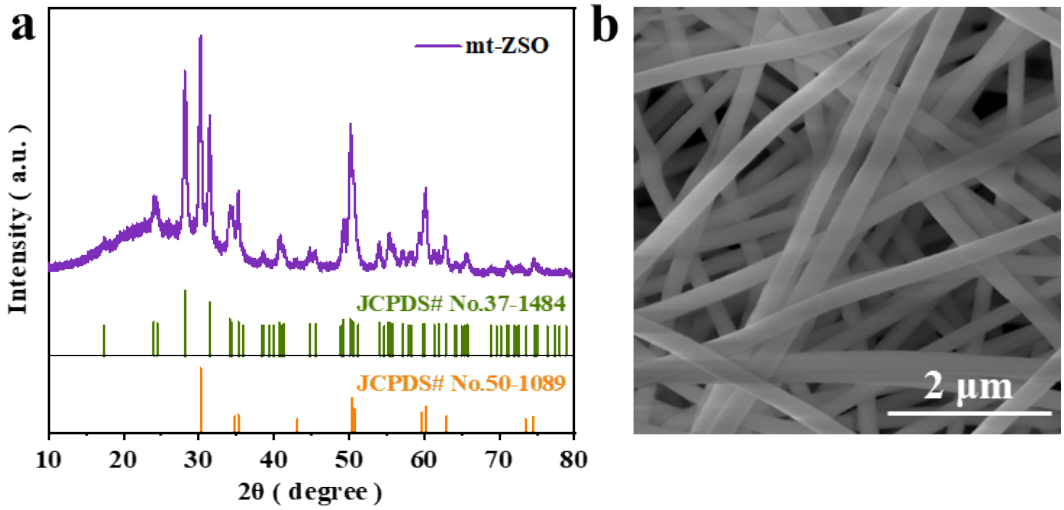

Fig. S2 (a) XRD pattern and (b) SEM image of mt-ZSO.

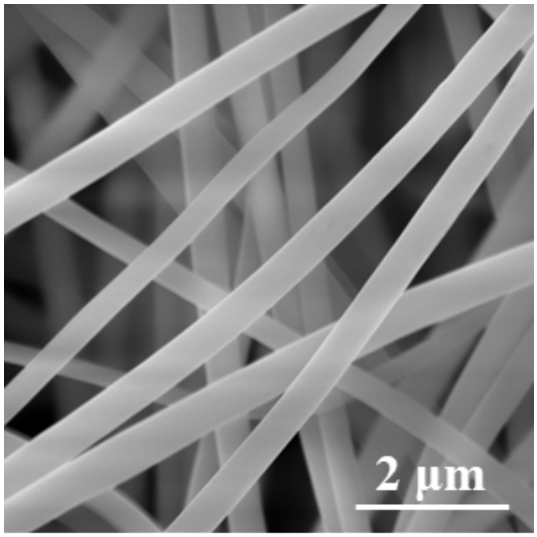

Fig. S3 SEM image of ZrO_2.

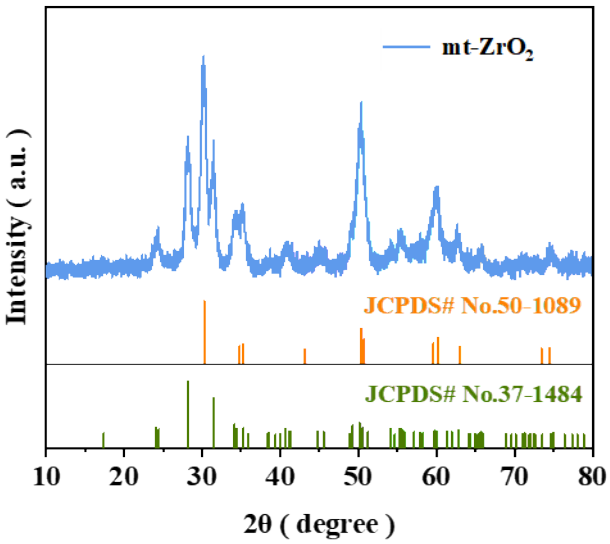

Fig. S4 XRD pattern of mt-ZrO_2.

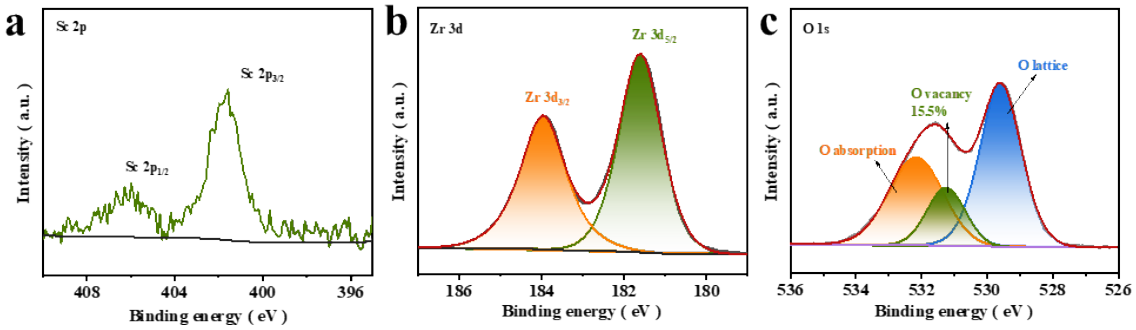

Fig. S5 XPS spectra of m-ZSO in the (a) Sc 2p, (b)Zr 3d and (c) O 1s region.

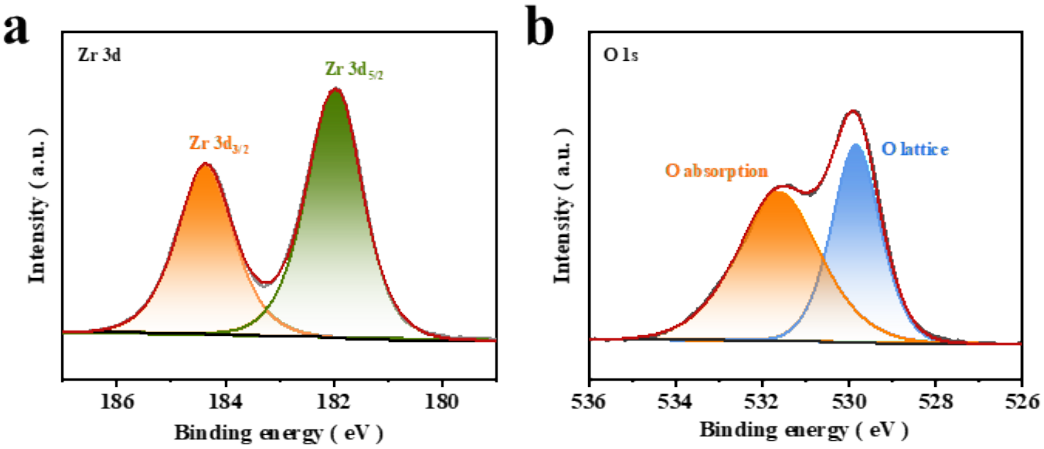

Fig. S6 XPS spectra of ZrO_2 in the (a)Zr 3d and (b) O 1s region.

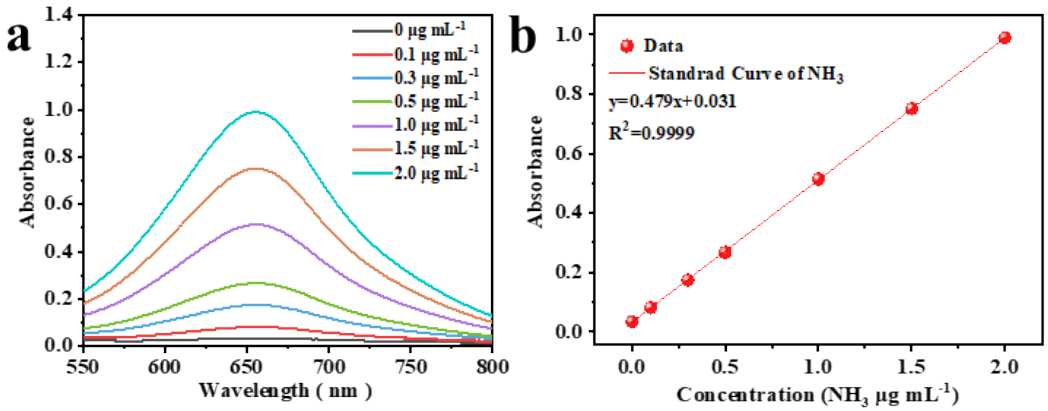

Fig. S7 (a) UV-vis absorption spectra of different concentrations of NH_3 stained with indophenol blue and (b) the corresponding calibration curve in 0.1 M PBS.

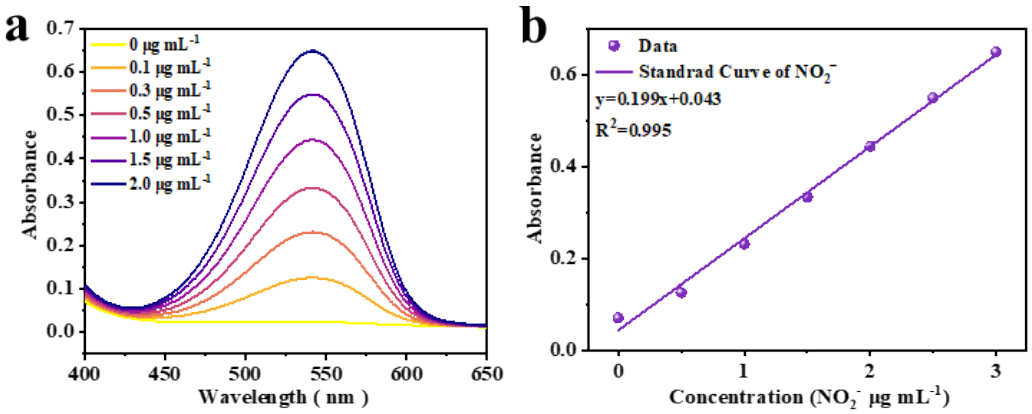

Fig. S8 (a) UV-vis absorption spectra of various concentrations of NO_2^- after sitting for 20 minutes and (b) the corresponding calibration curve in 0.1 M PBS.

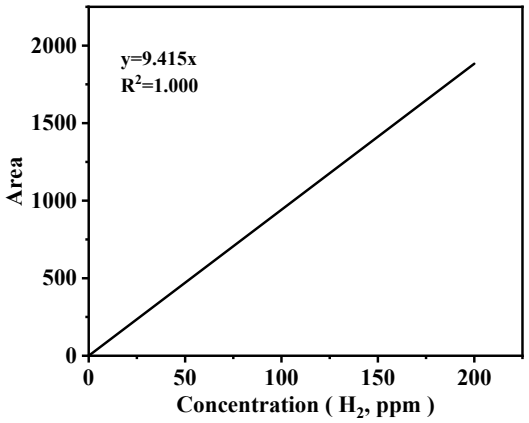

Fig. S9 The standard curve for calculating the H_2 yield.

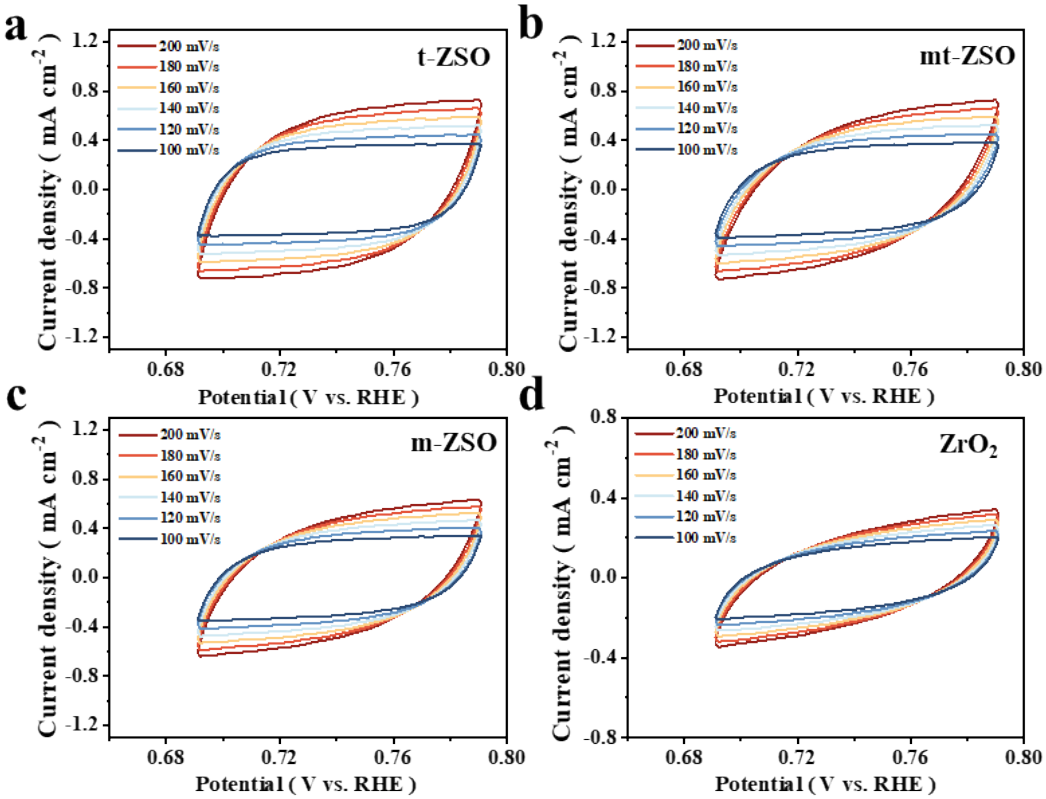

Fig. S10 CV curves of different scan rates of (a) t-ZSO, (b) mt-ZSO, (c) m-ZSO and (d) ZrO_2.

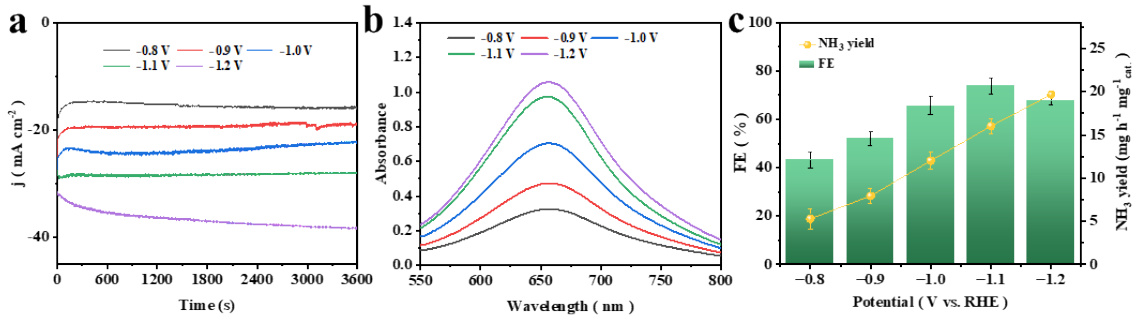

Fig. S11 (a) i-t curves for 1 h, (b) UV-vis absorption spectra at various potentials (-0.8 V to -1.2 V vs. RHE are diluted 20 times) and (c) NH_3 yield and FE of t-ZSO.

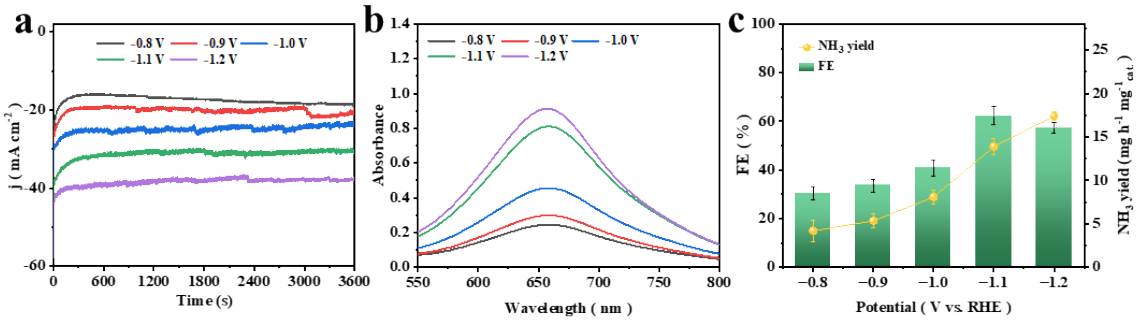

Fig. S12 (a) i-t curves for 1 h, (b) UV-vis absorption spectra at various potentials (-0.8 V to -1.2 V vs. RHE are diluted 20 times) and (c) NH_3 yield and FE of mt-ZSO.

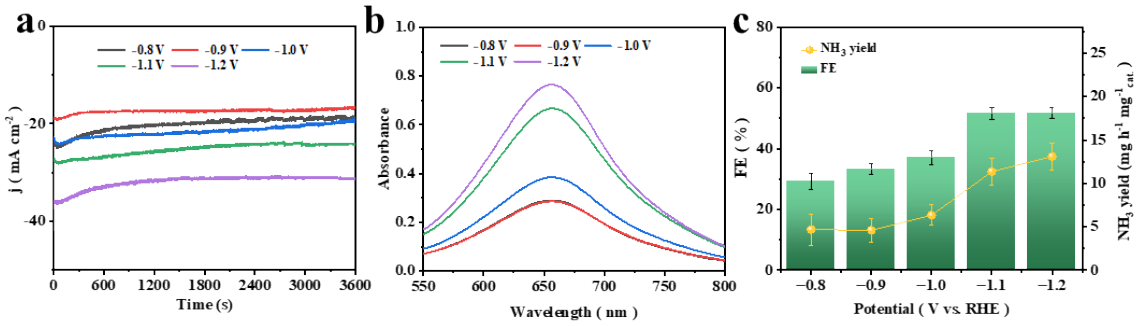

Fig. S13 (a) i-t curves for 1 h, (b) UV-vis absorption spectra at various potentials (-0.8 V to -1.2 V vs. RHE are diluted 20 times) and (c) NH_3 yield and FE of m-ZSO.

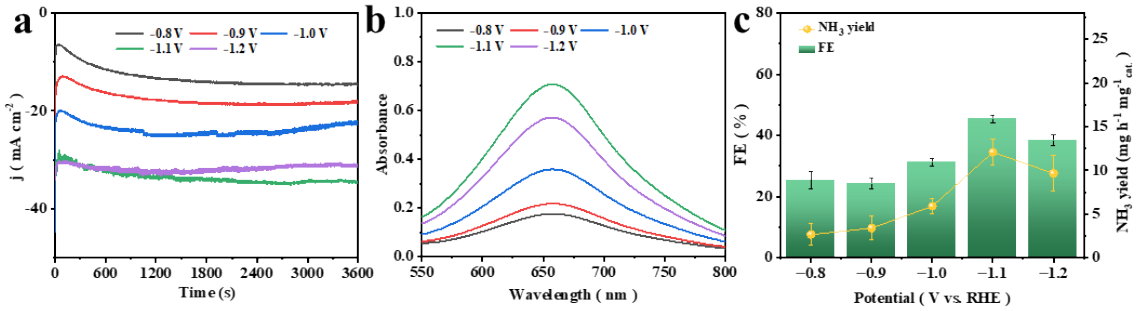

Fig. S14 (a) i-t curves for 1 h, (b) UV-vis absorption spectra at various potentials (-0.8 V to -1.2 V vs. RHE are diluted 20 times) and (c) NH_3 yield and FE of ZrO_2.

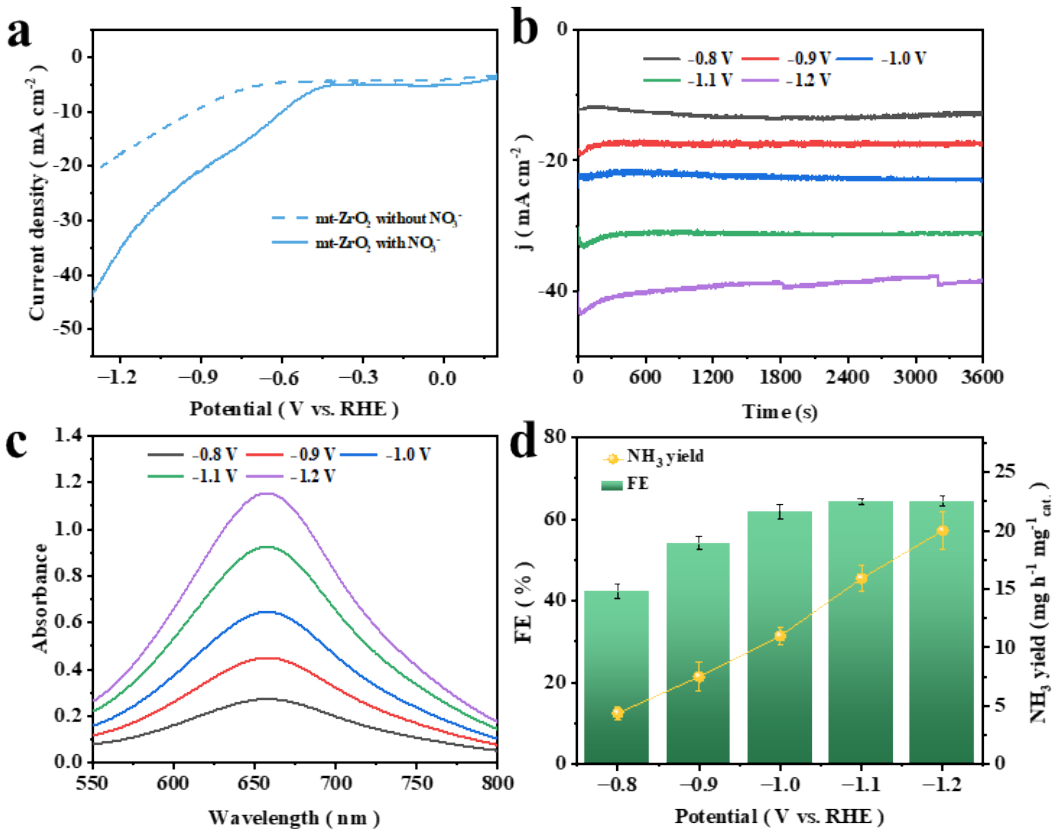

Fig. S15 (a) LSV curves in PBS with and without 0.1M NO_3^-, (b) i-t curves for 1 h, (c) UV-vis absorption spectra at various potentials (-0.8 V to -1.2 V vs. RHE are diluted 20 times) and (d) NH_3 yield and FE of mt-ZrO_2.

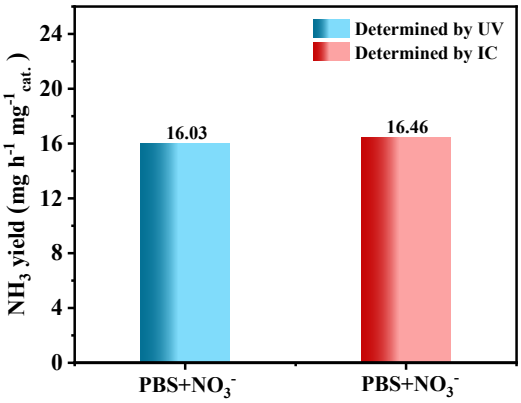

Fig. S16 The NH_3 yield rate was detected using the IC method and UV method after 1-h electrolysis in 0.1 M PBS with 0.1 M NO_3^- at -1.1 V over t-ZSO.

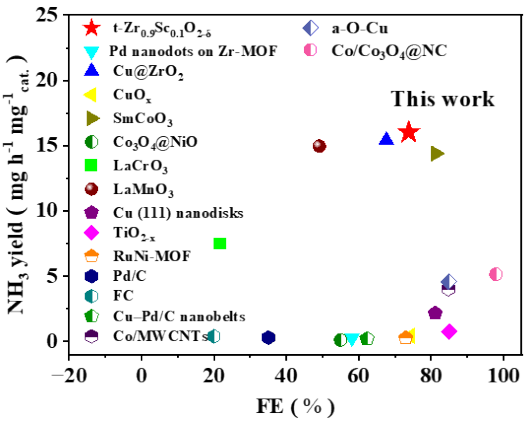

Fig. S17 Comparison of NH_3 yield and FEs of t-ZSO with some previously reported catalysts.

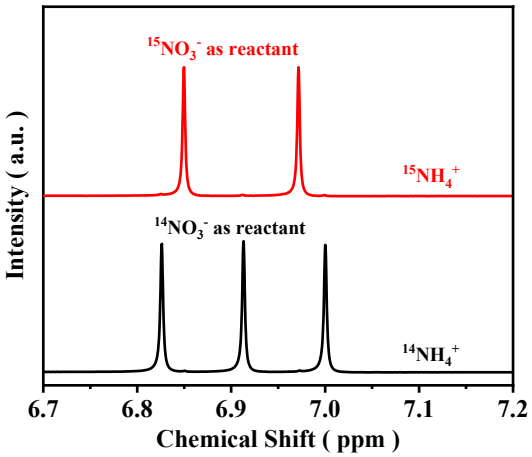

Fig. S18 ^{1}H NMR spectra of electrolyte after NITRR using $^{15}NO_3^-$ and $^{14}NO_3^-$ as nitrogen sources, respectively.

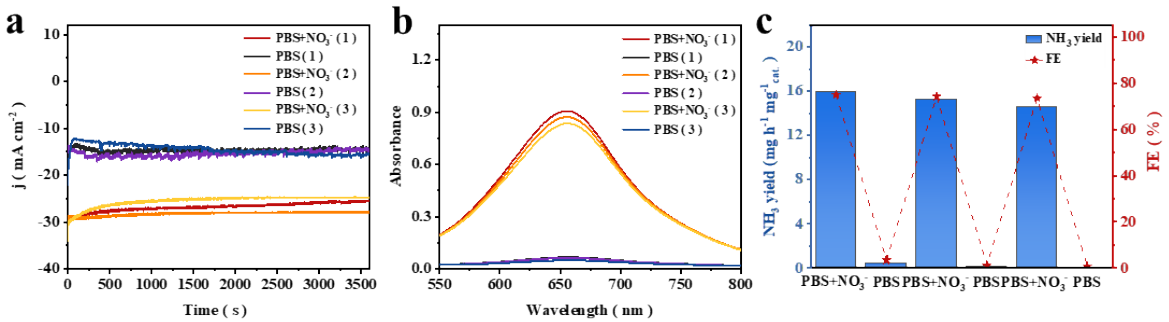

Fig. S19 (a) i-t curves for 1 h. (b) UV-vis absorption spectra of NH_3 and (c) NH_3 yields and FEs with alternating 1 h cycles in the PBS electrolyte with and without NO_3^- for t-ZSO.

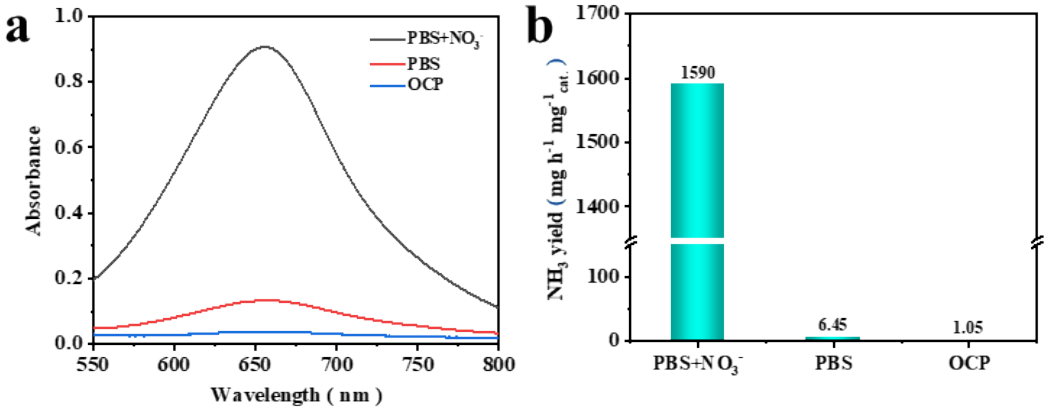

Fig. S20 (a) UV-vis absorption spectra of indophenol assays and (b) corresponding ammonia yield after 1-h electrolysis under different conditions for t-ZSO.

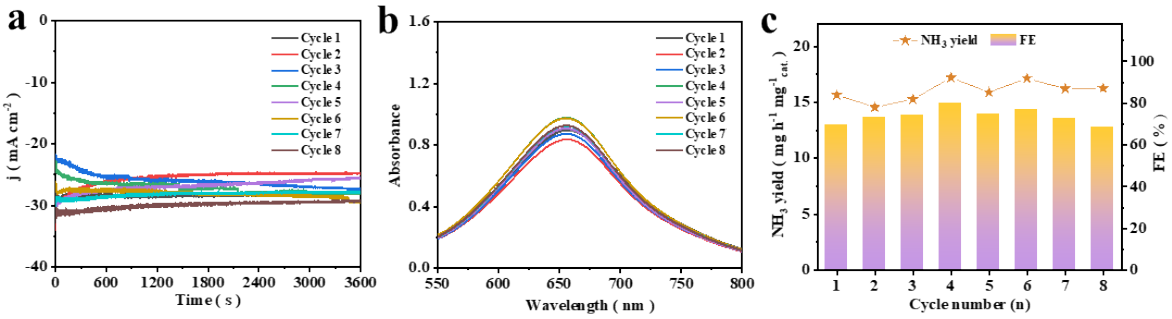

Fig. S21 (a) i-t curves for 1 h. (b) UV-vis absorption spectra of NH_3 of each cycle and (c) NH_3 yield and FE for 8 consecutive cycles of t-ZSO in 0.1 M PBS with 0.1 M NO_3^- electrolyte.

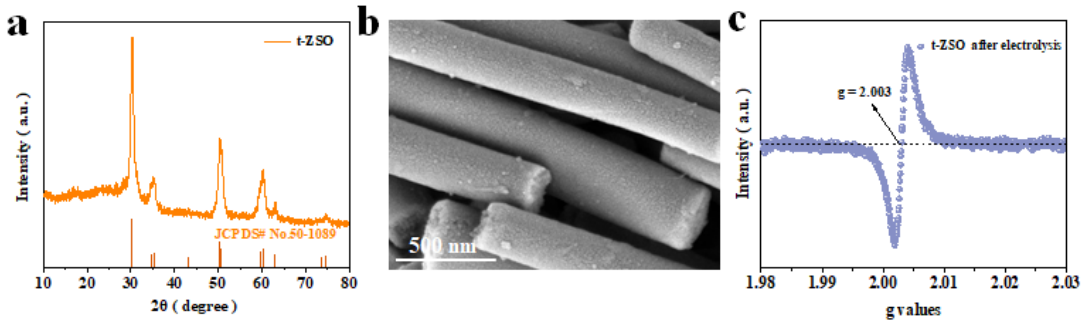

Fig. S22 (a) XRD pattern, (b) SEM image and (c) EPR spectrum of t-ZSO after electrolysis.

Table S1. Comparison of electrocatalytic NITRR performance for t-$Zr_{0.9}Sc_{0.1}O_{2-\delta}$ with other electrocatalysts under ambient conditions.

Catalysts	working voltage (V vs. RHE)	NH_3 yield (mg $h^{-1}mg^{-1}_{cat.}$)	FE (%)	Electrolyte	Ref.
t-$Zr_{0.9}Sc_{0.1}O_{2-\delta}$	**−1.1**	**16.03**	**73.84**	**0.1 M PBS + 0.1 M $NaNO_3$**	**This work**
Pd nanodots on Zr-MOF	−1.3	0.287	58.1	0.1 M Na_2SO_4 +500 ppm $NaNO_3$	9
Cu@ZrO_2	−0.7	15.4	67.6	0.1 M Na_2SO_4+1.6 mM $NaNO_3$	10
CuOx	−0.25	0.449	74.18	50 ppm KNO_3+0.1 M KOH	11
$SmCoO_3$	−1.0	14.4	81.3	0.1 M PBS +0.1 M $NaNO_3$	12
Co_3O_4@ NiO	−0.7	0.118	54.97	200 ppm NO_3^- +0.5 M Na_2SO_4	13
$LaCrO_3$	−1.0	7.48	21.7	1 M Na_2SO_4+0.5 M KNO_3	14
$LaMnO_3$	−1.0	14.96	49.1	1 M Na_2SO_4+0.5 M KNO_3	14
Cu (111) nanodisks	−0.5	2.16	81.11	0.1 M KOH + 0.01 M KNO_3	15
TiO_{2-x}	−1.0	0.765	85	0.5 M Na_2SO_4+ 50 ppm NO_3^-	16
RuNi-MOF	−1.2	0.274	73	0.1 M Na_2SO_4+50 mg L^{-1} $NaNO_3$	17
Pd/C	−0.2	0.307	35	0.1 M NaOH+ 0.02 M $NaNO_3$	18
FC	−0.65	0.405	20	0.05 M H_2SO_4+200 ppm KNO_3	19
Cu–Pd/C nanobelts	−0.4	0.221	62.3	0.1 M KOH + 0.01 M KNO_3	20

Co/MWCNTs	−0.16	4.03	84.72	0.1 M KOH + 0.1 M NO_3^-	21
a-O–Cu	−0.53	4.59	84.9	1 M KOH +200 ppm NO_3^-	22
Co/Co3O4@NC	−0.4	5.16	97.9	0.5 M Na_2SO_4 + 100 ppm NO_3^-	23

References

1. G. Kresse and J. Furthmüller, *Phys. Rev. B*, 1996, **54**, 11169.
2. G. Kresse and J. Furthmüller, *Comput. Mater. Sci.,*1996, **6**, 15-50.
3. G. Kresse and J. Hafner, *Phys. Rev. B*, 1994, **49**, 14251-14269.
4. M. Segall, P. J. Lindan, M. a. Probert, C. J. Pickard, P. J. Hasnip, S. Clark, M. Payne, *J. Phys.-Condes. Matter*, 2002, **14**, 2717.
5. P. E. Blochl, *Phys. Rev. B*, 1994, **50**, 17953-17979.
6. J. Perdew, J. Chevary, S. Vosko, K. Jackson, M. Pederson, D. Singh and C. Fiolhais, *Phys. Rev. B*, 1992, **46**, 6671-6687.
7. S. Grimme, J. Antony, S. Ehrlich and H. Krieg, *J. Chem. Phys.*, 2010, **132**, 154104.
8. H. Monkhorst and J. Pack, *Phys. Rev. B*, 1976, **13**, 5188-5192.
9. M. Jiang, J. Su, X. Song, P. Zhang, M. Zhu, L. Qin, Z. Tie, J. Zuo and Z. Jin, *Nano Lett.*, 2022, **22**, 2529-2537.
10. J. Xia, H. Du, S. Dong, Y. Luo, Q. Liu, J. S. Chen, H. Guo and T. Li, *Chem. Commun.*, 2022, **58**, 13811-13814.
11. J. Geng, S. Ji, H. Xu, C. Zhao, S. Zhang and H. Zhang, *Inorg. Chem. Front.*, 2021, **8**, 5209-5213.
12. P. Hu, S. Hu, H. Du, Q. Liu, H. Guo, K. Ma and T. Li, *Chem. Commun.*, 2023, **59**, 5697-5700.
13. Y. Wang, C. Liu, B. Zhang and Y. Yu, *Sci. China Mater.*, 2020, **63**, 2530-2538.
14. H. Zheng, Y. Zhang, Y. Wang, Z. Wu, F. Lai, G. Chao, N. Zhang, L. Zhang and T. Liu, *Small.*,2023, **19**, 2205625.
15. K. Wu, C. Sun, Z. Wang, Q. Song, X. Bai, X. Yu, Q. Li, Z. Wang, H. Zhang, J. Zhang, X. Tong, Y. Liang, A. Khosla and Z. Zhao, *ACS Mater. Lett.*, 2022, **4**, 650-656.
16. R. Jia, Y. Wang, C. Wang, Y. Ling, Y. Yu and B. Zhang, *ACS Catal.*, 2020, **10**, 3533-3540.
17. J. Qin, K. Wu, L. Chen, X. Wang, Q. Zhao, B. Liu and Z. Ye, *J. Mater. Chem. A.,* 2022, **10**, 3963-3969.
18. J. Lim, C. Liu, J. Park, Y. Liu, T. Senftle, S. W. Lee and M. Hatzell, *ACS Catal.*, 2021, **11**, 7568-7577.
19. Y. Li, S. Xiao, X. Li, C. Chang, M. Xie, J. Xu and Z. Yang, *Mater. Today Phys.*, 2021, **19**, 100431.
20. Z. Wang, C. Sun, X. Bai, Z. Wang, X. Yu, X. Tong, Z. Wang, H. Zhang, H. Pang, L. Zhou, W. Wu, Y. Liang, A. Khosla and Z. Zhao, *ACS Appl. Mater. Interfaces*, 2022, **14**, 30969-30978.
21. M. Ye, X. Jiang, Y. Zhang, Y. Liu, Y. Liu and L. Zhao, *Nanomaterials*, 2024, **14**, 102.
22. Q. Peng, D. Xing, L. Dong, Y. Fu, J. Lu, X. Wang, C. Wang and C. Guo, *J. Mater. Chem. A.*, 2024, **12**, 8689-8693.
23. L. Zhang, B. Zhang, Y. Hong, Y. You, Y. Zhou, J. Zhan, D. Alonzo Poole Iii and F. Yu, *Small*, 2024, 2402430.